Supporting Information

Xue et al. 10.1073/pnas.1412271111

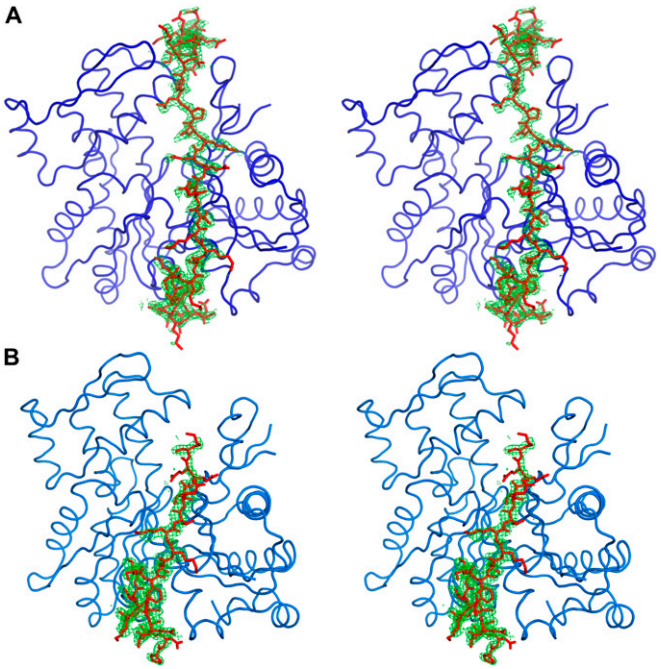

Fig. S1. Stereograms of the two structures of Tβ4:actin (cf. Fig. 1). (*A*) Structure of *Pichia* actin–Tβ4. (*B*) Structure of Tβ4–Cobl hybrid peptide in complex with rabbit skeletal muscle actin. In both *A* and *B*, actin is shown as a Cα trace; Tβ4 is shown as red sticks, with its composite omit 2Fo-Fc map contoured at 1.0 σ and colored green.

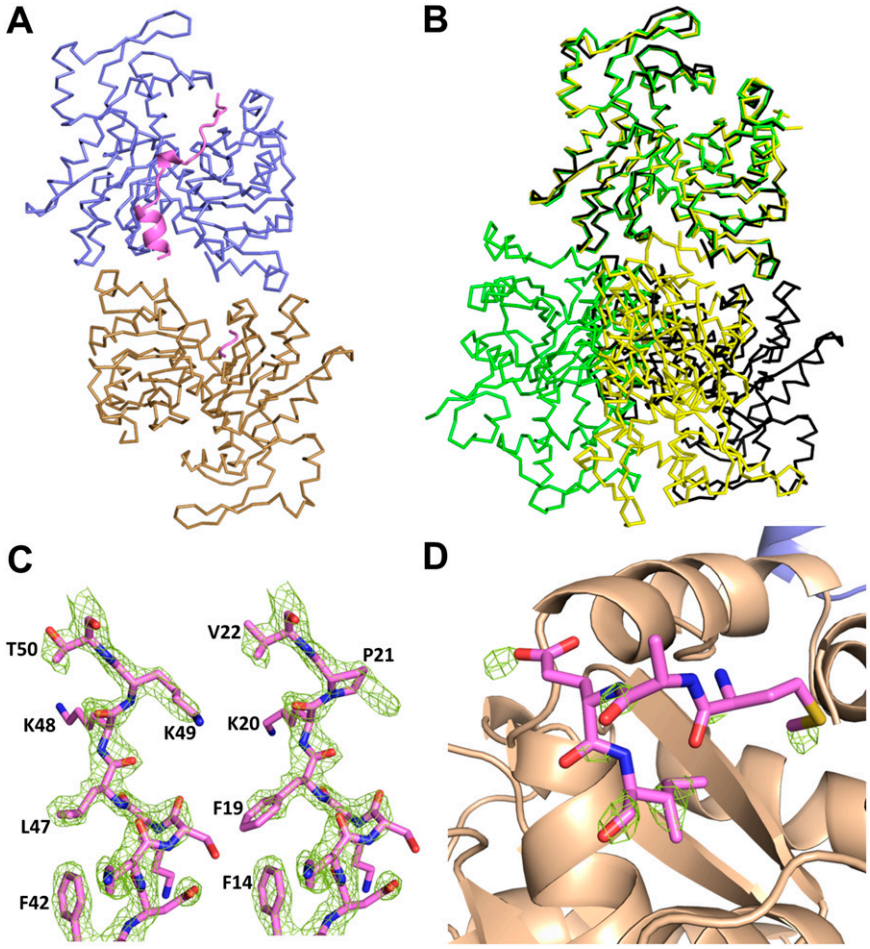

Fig. S2. Structure of the Tβ4–Cobl hybrid peptide in complex with rabbit skeletal muscle actin. (*A*) There are two actin molecules (blue and gold) in the asymmetric unit forming an antiparallel dimer. The hybrid peptide is in pink. (*B*) The antiparallel actin dimer reported here (black) is different from those induced by polylysine (PDB ID code 1LCU; yellow) and toxofilin (PDB ID code 2Q97; green). (*C*) Portion of the Fo-Fc omit map, contoured at 3.0 σ, shows unambiguously that the central portions of the visible residues on the surface of the first actin molecule are (*Left*) 42–50 (FDKSKLKKT) but (*Right*) not 14–22 (FDKSKFKPV) of the hybrid peptide. (*D*) The same omit map shows weak density at the barbed face of the second actin, which is assigned to residues 8–11 of the hybrid peptide.

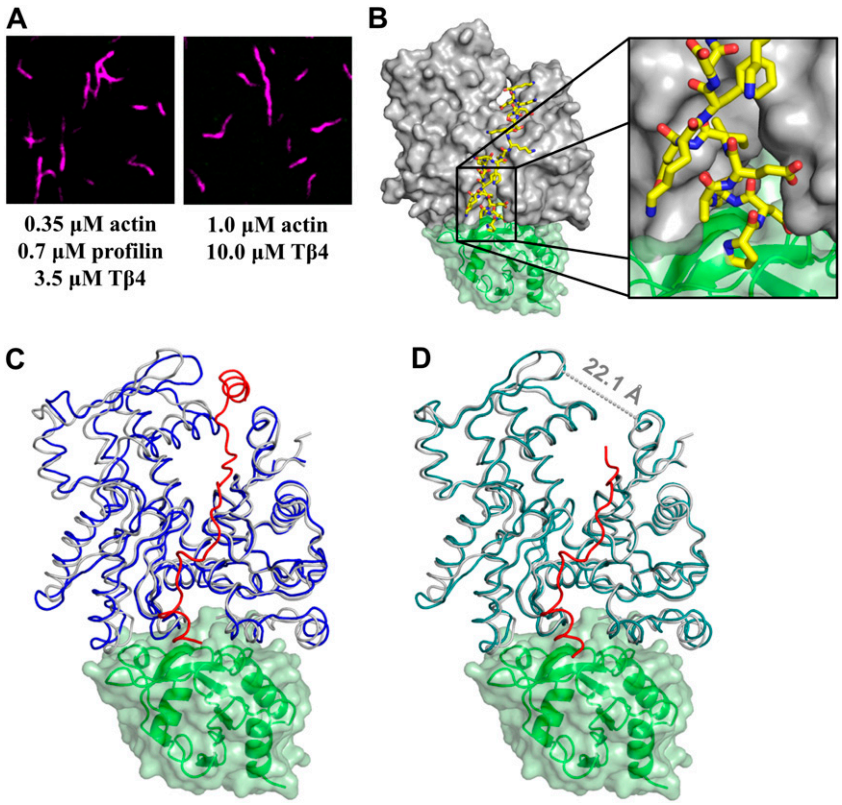

Fig. S3. Tβ4/profilin exchange of bound actin (cf. Fig. 2). (*A*) Competition between profilin and Tβ4 visualized by TIRF microscopy. Preformed filaments stained with rhodamine phalloidin (magenta) were immobilized on the surface of the flow cell. BODIPY FL-labeled G-actin (30% labeling; green) was then introduced into the flow cell. The absence of green filaments indicates that no new filaments were formed under the given conditions. (*B–D*) Model of the profilin:actin:Tβ4 ternary complex. The Tβ4:actin structures were superimposed onto the structure of profilin:actin (PDB ID code 2PBD). Actin and profilin from PDB ID code 2PBD are colored gray and green, respectively. Similar to the fully bound Tβ4 in Fig. 2*B*, the N-terminal helix of Tβ4N causes minimal steric clashes with profilin in *B*. The conformational differences between the actins in *C* are significant with fully bound Tβ4 and become less pronounced in *D* when the C-terminal helix of Tβ4 is released from the pointed face of actin. The distance mentioned in Fig. 1 is indicated by the dashed line for the profilin-bound actin in 2PBD.

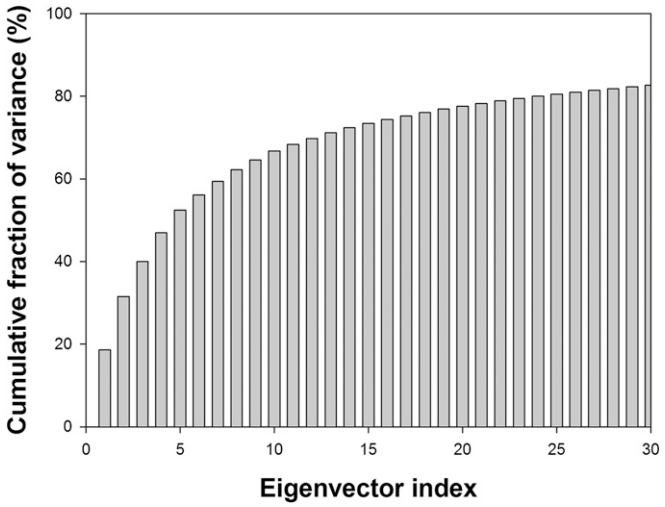

Fig. S4. Cumulative fraction of variance vs. eigenvector (PC) index. The histogram shows the percentage of the total variance of actin captured by the 30 first PCs.

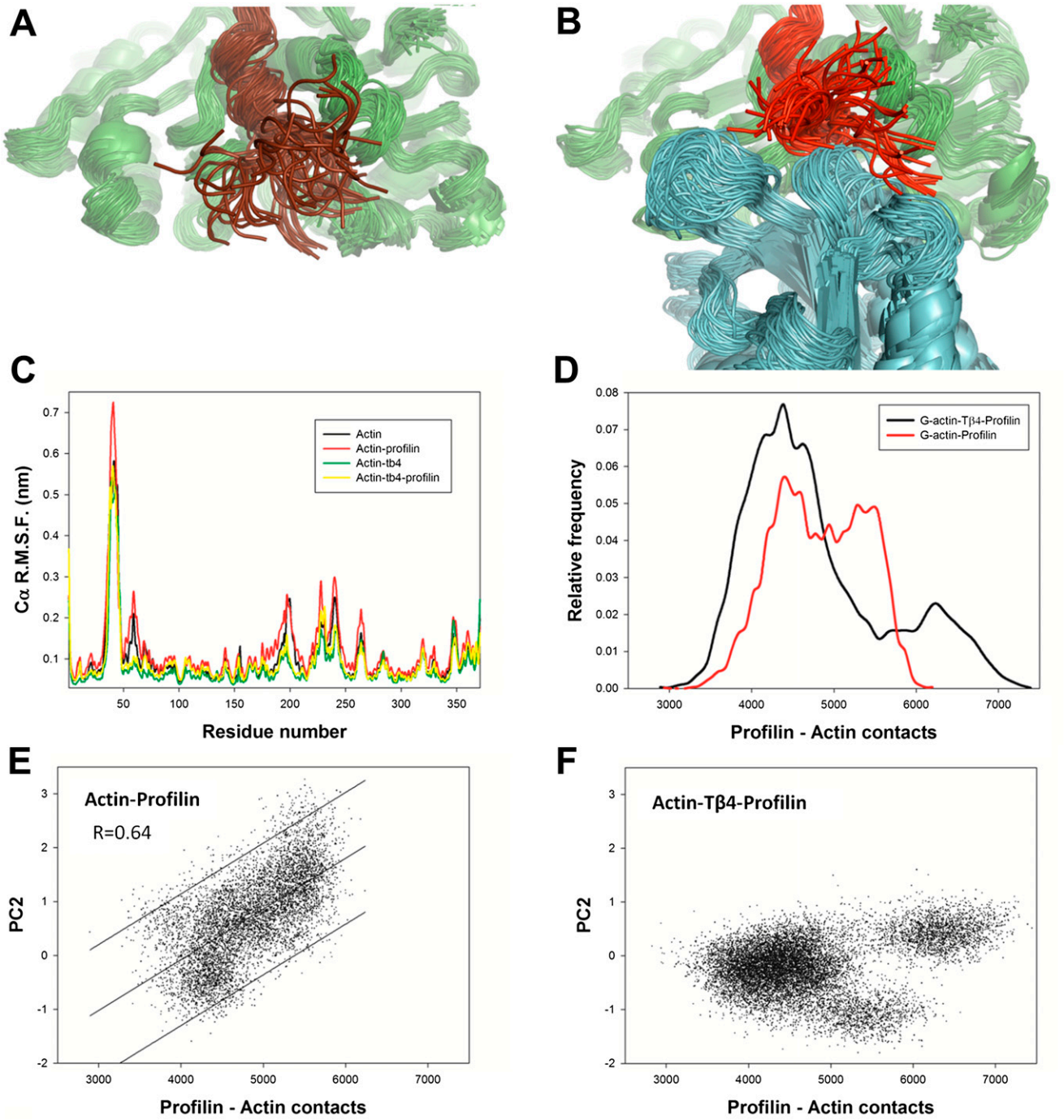

Fig. S5. Steric and allosteric components of profilin/Tβ4 exchange. (*A*) Superimposed MD snapshots taken at a 10-ns interval of the Tβ4:actin complex illustrating the conformational flexibility of Tβ4 N-terminal residues. (*B*) Superimposed MD snapshots taken at a 10-ns interval of the profilin:actin:Tβ4 complex showing the restricted conformational mobility of Tβ4 N-terminal residues within the tricomplex. (*C*) Root mean square fluctuations (RMSFs) of the actin molecule Cα atoms extracted from MD simulations of isolated actin, profilin:actin, Tβ4:actin, and profilin:actin:Tβ4. The RMSF was calculated on all Cα atoms after structural alignment of the protein backbone. Each curve corresponds to an average over three independent MD runs. (*D*) Comparison between the distribution of profilin:actin contacts in profilin:actin (red line) and profilin:actin:Tβ4 (black line). Contacts are defined as any atoms that are within a 0.6-nm distance of each other. (*E*) Plot of PC2 vs. the number of profilin:actin contacts in the profilin:actin complex showing a correlation between the two variables ($R = 0.64$). (*F*) Plot of PC2 vs. the number of profilin:actin contacts in the profilin:actin:Tβ4 complex showing clustering of the models in the low range of values for both PC2 and the number of profilin:actin contacts.

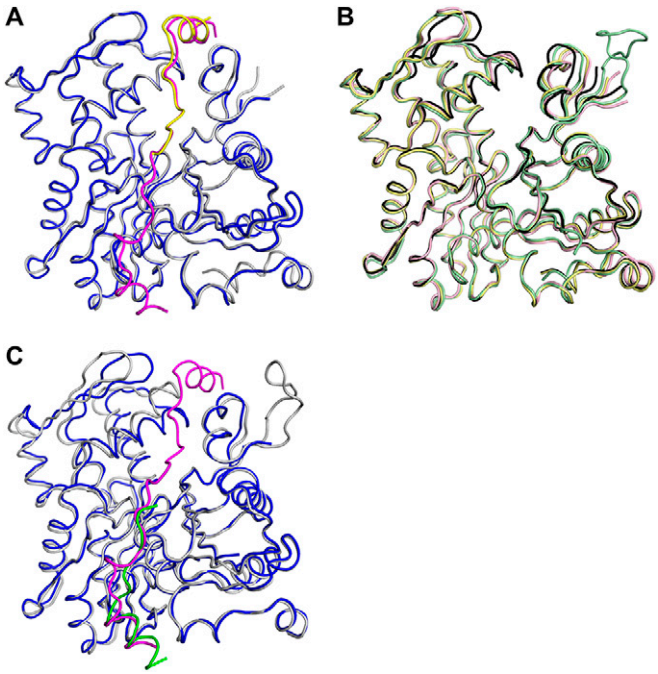

Fig. S6. The unique C-terminal α-helix of Tβ4. (*A* and *B*) The C-terminal α-helix of Tβ4 but not G1 induces the closure of the pointed face cleft of actin. (*A*) The structure of the *P.* (*Komagataella*) *pastoris* actin–Tβ4 hybrid closely resembles that of rabbit skeletal muscle actin bound to a chimera consisting of G1 fused to the C-terminal portion of Tβ4 (PDB ID code 1T44). The *Pichia* actin–Tβ4 hybrid is colored blue and magenta for its actin and Tβ4 portions, respectively. The rabbit skeletal muscle actin is colored gray, and the C-terminal portion of Tβ4 in the chimera is colored yellow. For clarity, the G1 in the chimera is not shown. (*B*) In the absence of the C-terminal α-helix of Tβ4, the pointed face cleft of actin remains open in G1:actin complexes. Actins from PDB ID codes 1YAG (*Saccharomyces cerevisiae* actin; pale green), 1P8Z (rabbit skeletal muscle actin; light pink), and 2FF3 (rabbit skeletal muscle actin; pale yellow) are compared with that from PDB ID code 1T44 (rabbit skeletal muscle actin; black). (*C*) The C-terminal α-helix of Tβ4 constitutes a major structural difference between Tβ4 and WH2. The *Pichia* actin–Tβ4 structure in Fig. 1*A* and the actin-bound structure of the WH2 motif of WASP are superimposed, with the fully bound Tβ4, WH2, and their bound actins shown in magenta, green, blue, and gray, respectively.

Table S1. Summary of MD simulations

System	No. of peptide chains	Nucleotide/cation	System size (atoms)	Total simulation time (μs)
Pichia actin	1	ATP/Ca^{2+}	50,375	0.869
Pichia actin–profilin	2	ATP/Ca^{2+}	73,288	0.669
Pichia actin–Tβ4	2	ATP/Ca^{2+}	55,638	1.150
Pichia actin–Tβ4–profilin	3	ATP/Ca^{2+}	76,466	1.200